

DISCRETE ELEMENT MODEL CALIBRATION USING MULTI-RESPONSES AND SIMULATION OF CORN FLOW IN A COMMERCIAL GRAIN AUGER



M. Z. Tekeste, M. Mousaviraad, K. A. Rosentrater

ABSTRACT. Grain augers are primary grain conveying equipment in agriculture. Quantitative prediction of dynamic grain flow in grain augers using discrete element modeling (DEM) has potential to support simulation-based engineering design of grain handling equipment. The objective of this study was to develop a DEM corn model using a multi-response calibration methodology and validation of combine-harvested corn flow in a commercial grain auger. Using a Latin hypercube design of experiment (DOE) sampling from four particle interaction DEM parameters values, 27 DEM simulations were generated for four DEM corn shape approximations (1-sphere, 2-spheres, 5-spheres, and 13-spheres) to create virtual DEM experiments of bucket-discharged and anchor-lifted angle of repose (AOR) tests. A surface meta-model was developed using the DEM interaction parameters as predictor variables, and normalized AOR expressed as a mean square error (MSE), i.e., the sum of square differences between DEM simulations and laboratory-measured AOR. Analysis of the MSE percentiles with lower error differences between DEM simulations and laboratory AOR and the computational effort required per simulation (h per simulation) showed that the 2-spheres DEM model had better performance than the 1-sphere, 5-spheres, and 13-spheres models. Using the best stepwise linear regression models of bucket AOR MSE (R^2 of 0.9423 and RMSE of 94.56) and anchor AOR MSE (R^2 of 0.5412 and RMSE of 78.02) and a surface profiler optimization technique, an optimized 2-spheres DEM corn model was generated. The DEM predicted AOR with relative errors of 8.5% for bucket AOR and 7.0% for anchor AOR. A DEM grain auger simulation used as a validation step also showed good agreement with the laboratory-measured steady-state mass flow rate (kg s^{-1}) and static AOR (degrees) of corn piled on a flat surface, with DEM prediction relative error ranging from 2.8% to 9.6% and from 8.55% to 1.26%, respectively.

Keywords. Corn, DEM, Discharge angle of repose, Discrete element modeling, Grain auger, Lift angle of repose.

Mechanical screw grain augers are commonly used for bulk grain conveyance in self-propelled combine harvesters, for loading and unloading grains from grain carts, as well as filling and emptying bins on the farm (Srivastava et al., 2006). Understanding and quantitative prediction of grain-to-grain and grain-to-equipment interactions are essential to support the development and validation of new grain handling equipment. The traditional product development cycle, including computer-aided design (CAD), physical prototyping, and functional tests in the laboratory and field, is often laborious, costly, and time-consuming. During machine-scale tests of grain handling systems, maintaining constant grain conditions, such as moisture content and grain quality, is often difficult and introduces undesirable measurement errors (Risius, 2014). Analytical performance prediction equations that were developed based on the dimensionless analysis (Robert

and Willis, 1962; Srivastava et al., 2006) are applicable for predicting volumetric conveyance efficiencies. Mathematical models that predict grain-equipment interactions have the potential to simulate the dynamic mechanical behavior and augment simulation-based design of bulk grain handling systems. In their experimental work on auger performance (e.g., volumetric and power requirements), Miao et al. (2014) and Robert (2015) indicated that experimental tests do not provide the dynamic flow from grain-to-grain and grain-to-rigid-body interactions. Computational tools have the potential to simulate the flow behavior of bulk solids and biomass materials in material handling equipment.

The discrete element method (DEM), a computational technique initially developed by Cundall and Strack (1979), has become a valuable engineering analysis tool for predicting the dynamic behavior of granular materials in agricultural grain handling equipment (Shimizu and Cundall, 2001; Owen and Cleary, 2009), mixing and milling processes (Kalala et al., 2005; Cleary, 2013; Kretz et al., 2016), and tillage-soil interactions (Asaf et al., 2007; Chen et al., 2013; Ucgul et al., 2014). As a mesh-free technique, DEM computes particle dynamics using discontinuous mechanics and has advantages over continuum and mesh-based techniques such as finite element analysis (FEA) and computational fluid dynamics (CFD), which have inherent problems asso-

Submitted for review in December 2017 as manuscript number PRS 12742; approved for publication by the Processing Systems Community of ASABE in August 2018.

The authors are **Mehari Z. Tekeste**, Assistant Professor, **Mohammad Mousaviraad**, Graduate Research Assistant, and **Kurt A. Rosentrater**, Associate Professor, Department of Agricultural and Biosystems Engineering, Iowa State University, Ames, Iowa. **Corresponding author:** Mehari Tekeste, 2331 Elings Hall, Iowa State University, Ames, IA 50011-1098; phone: 515-294-2464; e-mail: mtekeste@iastate.edu.

ciated with mesh distortion, numerical instability, and limited capability to simulate large strain deformations.

However, integrating DEM into simulation-based engineering analysis for the design of bulk grain handling equipment requires a standard technique for creating realistic approximations of irregular-shaped grains, a calibration methodology to determine the micromechanics contact model properties, and a validation methodology for simulating bulk grain handling applications. In general, DEM engineering workflow comprises: (1) efficient formulation of the particle simulation domain (particle size, DEM shape approximations, number of particles, and initial configurations of particles), (2) systematically scaling of the micromechanics model to accurately simulate bulk material behavior, and (3) efficient computing power. Computing power for DEM simulations has become affordable with the recent availability of high-performance computers and improved explicit time integration to run DEM on parallel computing cores (EDEM, 2014).

Researchers have used different approaches to select appropriate DEM microcontact models, define the particles, and generate material properties. For the determination of material properties, one approach that has been widely used is the direct measurement of DEM micromechanical properties, such as single grain-to-grain and grain-to-rigid-body (geometry) coefficients of restitution, coefficients of friction (sliding and rolling), and elastic Young's modulus. González-Montellano et al. (2012) used micromechanics measurement methods for individual corn and olive particles to generate the DEM particle density, Young's modulus, coefficients of restitution, and coefficients of friction. After limited success in predicting grain flow in a hopper, González-Montellano et al. (2012) introduced a trial-and-error approach for adjusting the DEM coefficients to improve prediction accuracy.

An alternative approach for direct measurement is calibration of the DEM model based on bulk behavior response. Coetzee and Els (2009a, 2009b) and Coetzee et al. (2010) calibrated their DEM model by running virtual direct shear and uniaxial compression tests. In their tests, they changed one DEM microparameter value while fixing the values of the remaining DEM parameters and virtually predicted the bulk grain Mohr-Coulomb failure parameters of cohesion and angle of internal friction. In their calibration process, Coetzee and Els (2009a, 2009b) applied a trial-and-error procedure by changing the DEM frictional coefficients and stiffness parameters to match the Mohr-Coulomb material properties. They reported a blade force DEM prediction error of 26% from simulations of blade-grain interactions. Coetzee et al. (2010) used uniaxial compression and angle of repose (AOR) calibration tests to improve the trial-and-error method for generating DEM properties. Coetzee (2017) recently conducted an extensive review of DEM calibration approaches based on previous studies and showed the calibration steps for a sensitivity study of one DEM parameter at a time. However, many of the calibration approaches explained by Coetzee (2017) still used a trial-and-error approach to determine each DEM parameter. A systematic integration of a calibration procedure and optimization of DEM properties for multi-response bulk behavior requires

further research, as most researchers have used trial-and-error approaches after sensitivity studies of DEM properties. The interaction effects of DEM parameters on bulk material behavior have not been used in DEM calibration approaches (Coetzee et al., 2017), even though experimental studies (Srivastava et al., 2006; Robert, 2015) have shown that grain flow in a grain auger is highly influenced by the interaction effects of friction coefficients between bulk granular particles and between particles and the screw and casing surfaces.

DEM shape approximation of granular materials has also been of interest in many studies (Coetzee, 2016; Markauskas et al., 2015; Stahl and Konietzky, 2011; Wiacek et al., 2012). In many DEM grain handling simulation studies, shape approximation was not included as a component of the calibration of the material properties, even though it appears to influence the rolling coefficient parameters and the computational effort. Developing a robust numerical methodology along with experimental testing for controlled, reproducible field-harvested grain conditions are important research challenges in using DEM for the design and performance analysis of grain handling equipment. In our previous work (Mousaviraad et al., 2017), a single AOR calibration and optimization approach was introduced to generate corn DEM friction parameter values and resulted in DEM simulations of grain auger mass flow rates with prediction errors of 27% and 29% for 250 and 450 rpm grain auger speeds, respectively. The prediction accuracy could be improved by using calibration for multiple-response AOR to investigate the effects of grain-to-grain, and grain-to-rigid-body interactions in quasi-static grain flow and by including such multi-response effects during the surface response optimization.

The overarching objectives of this study were to integrate DEM particle shape approximation into DEM material property estimation, develop a quantitative and multi-response DEM calibration technique, and validate the methodology by simulating corn flow through an auger. The specific objectives of this study were to (1) characterize the physical properties of field-harvested corn using standard measurement methods and simple bulk material flow tests, (2) develop a DEM corn model approximating the shape of corn kernels and calibrate the DEM material interaction properties using a Latin hypercube design of experiments (DOE) calibration technique, and (3) validate the DEM calibration technique by simulating the corn flow through an auger.

MATERIALS AND METHODS

CORN PHYSICAL CHARACTERIZATION

Material characterization for DEM calibration and validation was conducted on combine-harvested corn samples from the Iowa State University Agricultural and Agronomy farm in Boone, Iowa.

Corn Physical Properties

For measurement of the corn moisture content, particle density, and particle mass, the methods reported by Mousaviraad et al. (2017) were used. The moisture content was measured by the oven-drying method at 105°C for 24 h (ASABE, 2006). Corn kernels (sample size = 30) were randomly selected to measure five axial dimensions (height,

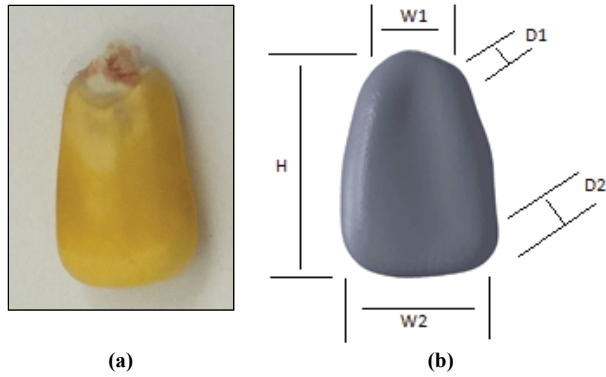


Figure 1. (a) Corn kernel and (b) CAD corn shape reconstructed from 3D scanned corn kernel (H = height, W1 = small width, W2 = large width, D1 = small depth, and D2 = large depth).

large width, large depth, small width, and small depth) using a digital caliper (0.01 mm resolution) (fig. 1a) and particle mass using a digital scale (0.01 g resolution). Particle density of the corn kernels was estimated according to ASTM (2000) by measuring the water volume displaced by a mass of kernels (sample size = 30) immersed in a 1 mm graduated cylinder (100 mm³ capacity). Bulk density was measured by loosely filling a bucket with a known mass of corn (3 kg). A representative corn kernel was 3D scanned and reconstructed in SolidWorks CAD software to generate an approximate 3D corn shape (fig. 1b).

Coefficient of Restitution

The coefficient of restitution for particle-to-particle and particle-to-rigid-body interactions was measured by dropping a single kernel from a vertical height (h_{initial}) of 200 mm onto a cylinder randomly filled with corn and onto a flat surface geometry. The maximum height (h_{max}) of the rebounded kernel after impacting the surfaces was measured from video captured at 240 frames s⁻¹ (fps) with a 5 mm resolution ruler in the background. By analyzing the video frames, the maximum kernel height (h_{max}) for each test was estimated. The coefficients of restitution (e) for the corn-to-corn ($e_{\text{corn:corn}}$)

and corn-to-geometry ($e_{\text{corn:geometry}}$) interactions were estimated using $e = \sqrt{h_{\text{max}}/h_{\text{initial}}}$ according to Zhang and Vu-Quoc (2002).

BULK ANGLE OF REPOSE

The bulk AOR is defined as the angle of a piled bulk material with respect to a horizontal plane (Boac et al., 2010; Mohsenin, 1986). Schulze (2007) described several methods for measuring bulk AOR, including poured, drained, and dynamic AOR. Some of the factors that affect bulk AOR are sliding and rolling frictional forces interacting within the granular pile and free-surface flow (Walton and Braun, 1993), particle shape, particle size distribution, grain moisture content, and base plate material properties (Boac et al., 2010). For calibration of DEM granular flow in material handling equipment, such as grain augers, both grain-to-grain and grain-to-rigid-body frictional (sliding and rolling) resistances influence the dynamic grain flow and equipment performance (Robert, 2015). In this study, two measurement methods were conducted: bucket-discharged AOR and anchor-lifted AOR. The bucket-discharged AOR test approximates the drained AOR (Schulze, 2007), which seems to be influenced by grain-to-grain and grain to-rigid-body interactions as grains slide along the bucket walls. The anchor-lifted AOR test was conducted to quantify the effects of grain-to-grain friction coefficients with minimum effects from grain-to-rigid-body interactions on the AOR. For DEM calibration purposes, these two simple tests were considered to provide multiple responses because the formation of AOR is affected by grain-to-grain and grain-to-rigid-body interaction parameters.

Bucket-Discharged AOR Test

Bucket AOR (α_{bucket}) is the fall or drained angle formed after loosely filled and unconsolidated corn grains in a bucket are discharged onto a flat plate (fig. 2, left). The bucket dimensions, material type, and testing procedure were similar to those reported by Mousaviraad et al. (2017). A box (height = 200 mm, length = 250 mm, and width =

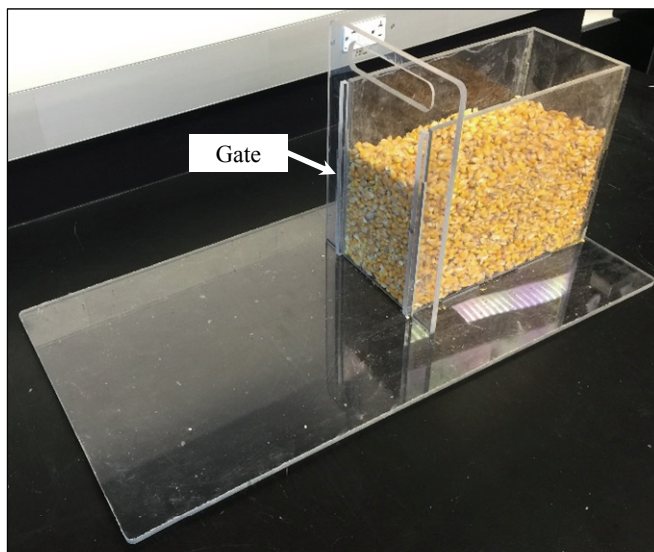


Figure 2. (left) Simple experiments for bucket-discharged AOR (α_{bucket}) and (right) anchor-lifted AOR (α_{anchor}) in which an anchor (b) was lifted to form an angle of repose (AOR) from a cylinder (a) loosely filled with corn.

120 mm) was fabricated from acrylic sheet. A transparent 5 mm × 5 mm grid was carefully applied to the length (250 mm) and height (200 mm) of the bucket. The initial loosely filled corn bulk density was 520 kg m⁻³. A gate with a width of 120 mm was opened vertically at an approximate speed of 5 m s⁻¹, and the corn particles formed an AOR along the bucket length. The bucket AOR test was replicated five times. After AOR formation along the bucket length and height, the corn height was estimated for each of the 5 mm × 5 mm grid cells along the bucket length (0 to 250 mm). The corn height (h_{exp}) was used to calculate a standardized error estimate for DEM calibration and the bucket AOR.

Anchor-Lifted AOR Test

A second test was constructed to measure the AOR as grains were lifted from the loosely filled material. The test for anchor-lifted AOR (α_{anchor}) consisted of a cylinder with a diameter of 190 mm and height of 110 mm, and an anchor consisting of 15.7 mm diameter cylindrical tube, a square flat bottom (101 mm), and 90° wall (height of 12.5 mm) glued to the square flat bottom (fig. 2, right). To minimize the corn-to-wall friction coefficient, the height of the square bottom was set to the mean corn height measured using a digital caliper. The acrylic material and grain filling method were similar to the bucket-discharged AOR test. The anchor was pulled up at approximately 30 mm s⁻¹, and the anchor AOR (α_{anchor}) was estimated using an image processing procedure in Matlab (ver. 2016a) for the digitally captured images. The grain flow behavior that formed the free-surface AOR was affected by the grain-to-grain angle of internal friction, with limited influence from grain-to-rigid-body effects. The bucket and anchor AOR tests together provided multi-response behaviors of grain flow as influenced by grain-to-grain and grain-to-geometry rigid-body friction behaviors.

GRAIN AUGER TEST

A commercial grain auger (Westfield Co., Boone, Iowa), with total auger length of 327 mm, outer tube (shell) diameter of 100 mm, grain auger diameter of 90 mm, grain auger

shaft of 50 mm, pitch length of 100 mm, and intake length of 206 mm, was used to measure corn flow through a grain auger (fig. 3a). The dimensions of the grain auger are shown in figure 3b. Grain flow tests were conducted at two rotational speeds (250 and 450 rpm) at 0° inclination from horizontal. The rotational speed was first set to the target value. After the grain auger was operating at the desired rotational speed, corn was fed continuously into the auger intake to provide an approximate mass flow rate of 20 kg s⁻¹. While the corn was conveyed through the auger, additional corn was added to the intake to maintain an approximately constant mass flow rate. The transient corn mass discharged from the auger was measured at a 4 Hz sampling rate using a digital scale (0.2 kg mass resolution). A non-contact laser tachometer (HHT13, class 3R visible laser, Omega Engineering, Norwalk, Conn.) was used to measure the rotational speed during the grain conveying tests. Similar to the data collection for mass flow versus time, tests were also conducted at a 0° auger inclination angle and two rotational speeds (250 and 450 rpm) to estimate the poured AOR as corn was discharged from the auger and fell onto a flat steel surface.

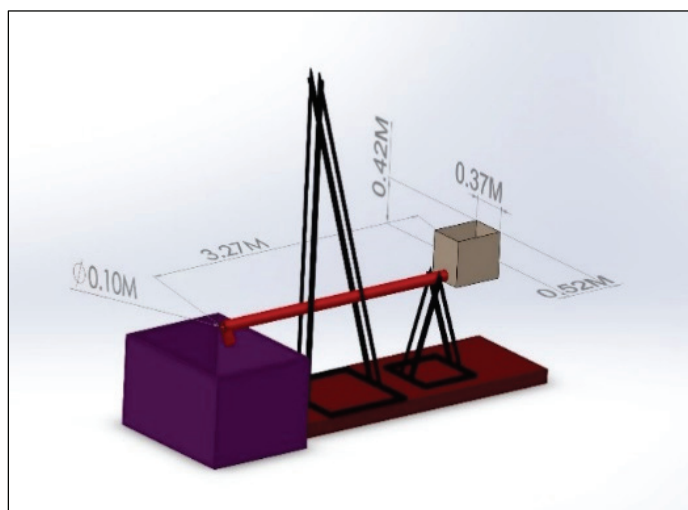
DEM CALIBRATION APPROACH

DEM Contact Model Parameters

The Hertz-Mindlin contact model is one of the most commonly used DEM contact models for non-cohesive particles. The Hertz-Mindlin model is a non-linear spring elastic contact model that defines the constitutive relationships of force and overlap using normal and tangential spring stiffness parameters in the normal and tangential contact overlaps between particles. Frictional slip is allowed in the tangential direction using a slider spring response and is limited to the maximum value determined by Mohr-Coulomb friction behavior. Both normal and tangential forces have damping components in which the damping is related to the coefficient of restitution. The Hertz-Mindlin contact model with rolling friction, after Tsuji et al. (1992), was used in EDEM 2.7 (EDEM, 2014).



(a)



(b)

Figure 3. (a) Commercial grain auger at 0° inclination for the laboratory test setup and (b) 3D CAD drawing. The feed intake, the auger tube with a helical screw, the shaft, and the discharge bucket as shown in the CAD drawing were reproduced in EDEM 2.7.

EDEM 2.7 (EDEM, 2014), a commercial DEM code, was used to create DEM corn particles and run the DEM simulations for the calibration and validation experiments. The corn particles were assumed to be frictional and non-cohesive. The EDEM parameters needed to define corn DEM using the Hertz-Mindlin (no slip) contact model included: (1) the corn particle shape (particle radius and position of individual sphere elements), (2) material property parameters (Poisson's ratio, shear modulus, and particle density), and (3) material interaction properties, including particle-to-particle coefficient of restitution, particle-to-particle coefficient of static friction, particle-to-particle coefficient of rolling friction, particle-to-rigid-wall (rigid body) coefficient of restitution, particle-to-wall (rigid body) coefficient of static friction, and particle-to-wall (geometry) coefficient of rolling friction.

DEM Corn Particle Definition

For the DEM corn shape approximation, four DEM corn shapes were created in EDEM 2.7, including one sphere (1-sphere), two clumped spheres (2-spheres), five clumped spheres (5-spheres), and 13 clumped spheres (13-spheres) (fig. 4). The mean equivalent geometric diameter of a corn kernel (sample size =30) was used as the diameter for the 1-sphere DEM corn shape (radius of 4 mm). The geometric mean was calculated from the corn kernel height, large width, and small width measurements. The 2-spheres DEM corn model approximately matched the aspect ratio calculated from the height and maximum width of a corn kernel

(radius of 2.54 mm for the top sphere and 4 mm for the bottom sphere). The 5-spheres DEM corn model approximately matched the height, maximum width, and maximum depth of a corn kernel (radius of 2.84 mm for the top sphere, 2.7 mm for the middle spheres, and 2.54 mm for the bottom spheres). The 13-spheres DEM corn model approximately matched the height, maximum width, minimum width, maximum depth, and minimum depth of a corn kernel (radius of 2.5 mm for the top sphere and 2 mm for the other spheres).

DEM Material Properties Initialization

The values of Poisson's ratio and shear modulus for corn and the rigid body (acrylic) were obtained from the literature (Boac et al., 2010). Laboratory-measured values of corn particle density, the corn-to-corn coefficient of restitution, and the corn-to-wall (acrylic) coefficient of restitution were assigned to each DEM corn model. After the DEM particles were generated in EDEM 2.7, reproducing the calibration experiments in the bucket and anchor AOR tests, the DEM particle density values were adjusted to match the DEM initial bulk density to the laboratory-measured initial bulk density. Adjustment of particle density to match bulk density has also been used by other researchers (Coetzee, 2017). The DEM interaction parameters, including the coefficients of corn-to-corn static friction (CC_stat), corn-to-corn rolling friction (CC_roll), corn-to-acrylic static friction (CA_stat), and corn-to-acrylic rolling friction (CA_roll), were identified as independent parameters for the sensitivity study. The low and high settings of the four interaction parameters were

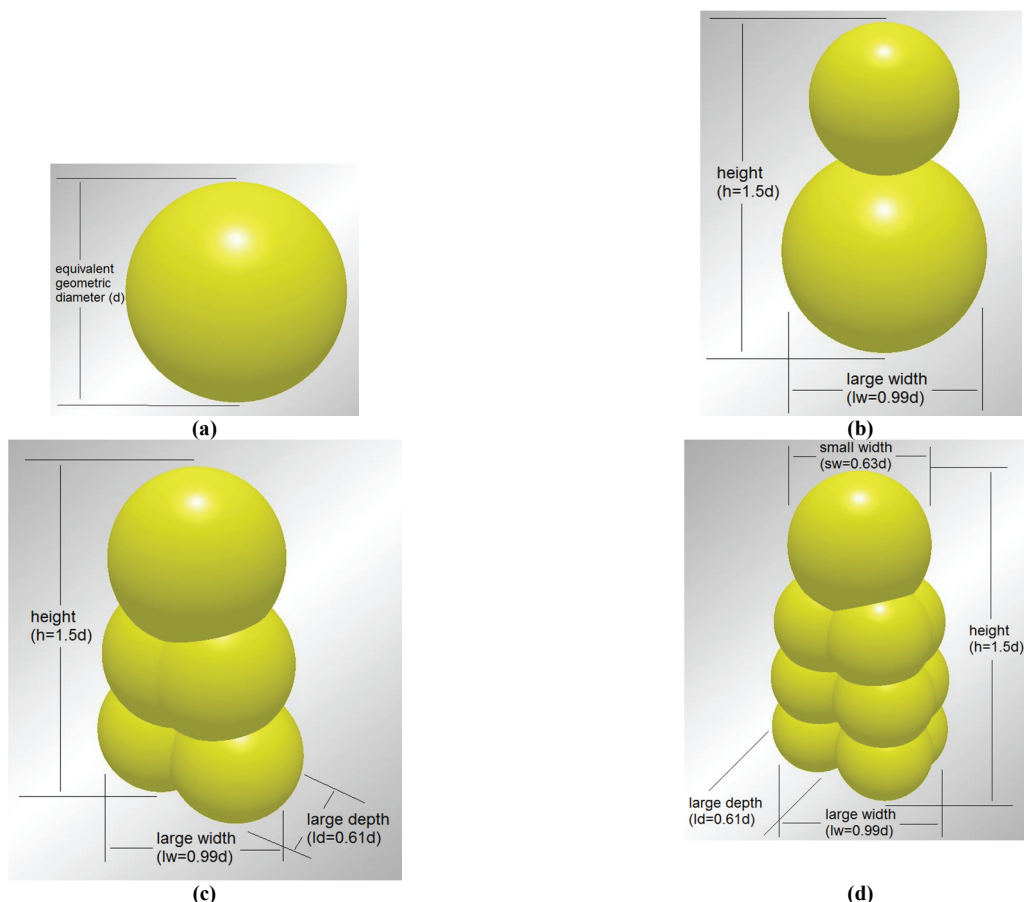


Figure 4. EDEM corn shape approximations: (a) 1-sphere ($d = 8.0$ mm), (b) 2-spheres, (c) 5-spheres, and (d) 13-spheres.

used to generate 27 experimental combinations using a Latin hypercube DOE. The remaining DEM material and interaction properties were fixed to the laboratory-measured values and literature estimates. The low and high values of the static frictional interaction parameters of corn and acrylic (CC_stat and CA_stat) were obtained from previous DEM literature (Boac et al., 2010; Coetzee and Els, 2009a, 2009b; González-Montellano et al., 2012). Initial DEM simulations of bucket AOR were run to estimate low and high values for the coefficients of corn-to-corn rolling friction (CC_roll) and corn-to-acrylic rolling friction (CA_roll). For our study, the AOR was assumed to be sensitive to the four DEM interaction parameters (CC_stat, CC_roll, CA_stat, and CA_roll) and was also assumed to influence the grain flow behavior in the auger strongly.

Using the Latin hypercube DOE consisting of 27 combinations of the four DEM parameters (CC_stat, CC_roll, CA_stat, and CA_roll), a total of 216 EDEM simulation input decks were generated. The 216 ($4 \times 2 \times 27$) EDEM simulation input decks were created for the four DEM corn particle shapes, the two calibration experiments, and the 27 combinations of the four DEM friction coefficients.

DEM Sensitivity and Optimization Criteria

After generating DEM simulations for the 27 experimental combinations in EDEM 2.7, mean square error (MSE) variances (mm^2) were estimated from the square of the differences in the AOR response variables from the DEM simulations and laboratory experiments. The MSE from the bucket AOR test was calculated using equation 1:

$$\text{MSE}_{\text{BucketAOR}} = \sum_{i=1}^N \frac{(h_s - h_{\text{exp}})^2}{N} \quad (1)$$

where $\text{MSE}_{\text{BucketAOR}}$ is the sum of the square of the difference in the height of corn from the DEM simulation (h_s) and from the experiment (h_{exp}) at every grid cell from $i = 1$ to N along the bucket length. Similar to the procedure used in the bucket-discharged AOR test, the height of corn (h_s) from the DEM simulation was extracted from the $5 \text{ mm} \times 5 \text{ mm}$ grid cells along the length of the bucket.

The MSE (deg^2) from the anchor AOR test was calculated using equation 2:

$$\text{MSE}_{\text{AnchorAOR}} = \sum_{i=1}^N \frac{(\text{AOR}_s - \text{AOR}_{\text{exp}})^2}{N} \quad (2)$$

where $\text{MSE}_{\text{AnchorAOR}}$ is the mean square error between the anchor AOR test and the DEM simulation, AOR_s is the AOR from the DEM simulation, AOR_{exp} is the AOR from the anchor-lifted AOR test, and $N = 4$ is the number of sampling positions.

The mean square error (MSE), as a function of the error between the AOR tests and DEM simulations, was used to statistically analyze the influences of the DEM interaction parameters on the coefficients of friction, approximate the surface response meta-models, and optimize the DEM properties (CC_stat, CC_roll, CA_stat, and CA_roll) with minimum prediction errors based on the bucket and anchor AOR tests.

Validation of DEM Grain Flow Simulation

After the DEM calibration process using multi-responses from the two AOR tests was completed, DEM simulation of the auger system was conducted as the validation process. Grain augers are commonly used in bulk material handling, with a wide range of applications. The working principle of a grain auger forces the material grains to rotate and slide against each other and the equipment surfaces. Granular materials also experience collisions and accelerations while passing through an auger. The complex, dynamic behavior of granular material inside a grain auger makes such a system a suitable application for validation of DEM models. After systematic DEM calibration, simulation of the grain auger with corn was assumed to validate the robustness of the DEM methodology applicable to grain handling equipment.

In the DEM simulation, the auger was set at a horizontal position (0° incline), and tests were performed at 250 and 450 rpm rotational speeds, similar to the laboratory experiments. The corn-to-steel (auger geometry) sliding and rolling coefficients were estimated as the AOR optimized corn-to-acrylic coefficients (static and rolling) and multiplied by 1.58, a value estimated from laboratory-measured corn-to-acrylic and corn-to-steel coefficient ratios after Boac et al. (2010) and González-Montellano et al. (2012). The grain auger geometry and the dynamics of the experimental setup (fig. 3b) were modeled in EDEM 2.7. The steady-state mass flow rate and the AOR of corn discharged onto a flat surface, as measured in the laboratory and simulated by DEM, were statistically compared.

Computer Setup for DEM Simulations

A Dell computer with an 8-core Intel Xeon E3-1271 3.6 GHz CPU, NVIDIA Quadro K60 graphic card, and 16 GB of RAM was used for the DEM simulations. The EDEM simulation settings were a time step of $5\text{e-}6$ s, a grid cell three times the minimum sphere radius (EDEM, 2014), and 8-core processors. Each simulation was run for 60 s, and output data were exported every 0.05 s. The CPU time for each DEM simulation was also recorded to compare the computational effort required for the DEM runs.

DATA ANALYSIS

Statistical analysis was performed using a stepwise statistical GLM procedure in JMP Pro 11.0.0 (SAS Institute Inc., Cary, N.C.) to identify the main factors and two-way interaction effects of the DEM material properties on the MSE from the bucket and anchor AOR tests for each DEM corn shape approximation. A stepwise regression technique applying the criterion of p-values between 0.05 and 0.1 was used to enter and leave the predictor parameter effect estimates in the regression model. A stepwise regression meta-model with a minimum root means square error (RMSE) and maximum coefficient of determination (R^2) was used for the surface response optimization. Using 5,000 independent combinations of the four DEM parameter values and the best meta-model to predict MSE, the prediction surface desirability profiler procedure in JMP Pro 11.0.0 (SAS Institute Inc., Cary, N.C.) with the objective of minimum MSE for both the bucket and anchor AOR tests was used to obtain the optimized DEM parameter values.

Table 1. Physical properties of combine harvested corn samples.^[a]

Property	Mean	Min.	Max.
Dimensions			
Height (mm)	12.57	11.26	14.54
Large width (mm)	7.99	6.83	9.84
Large depth (mm)	4.89	3.71	7.26
Small width (mm)	5.07	3.45	7.26
Small depth (mm)	3.23	2.93	4.04
2D aspect ratios			
Height/large width	1.59	1.24	2.00
Height/large depth	2.67	1.59	3.55
Corn kernel mass (g)	0.35	0.20	0.47
Moisture content (% d.b.)	15.2	14.9	16.1
Particle density (kg m ⁻³)	1273	1178	1363
Bulk density (kg m ⁻³)	771	754	801

^[a] Values were determined from 30 replicates except for bulk density, which was determined from five replicates.

RESULTS AND DISCUSSIONS

CORN PHYSICAL PROPERTIES

Descriptive statistics (means and standard deviations) for the corn kernel dimensions, aspect ratios, and material properties are presented in table 1 (Mousaviraad et al., 2017). The mean corn particle density was within the ranges reported by Boac et al. (2010) and González-Montellano et al. (2012). The dimensional measurements matched the values obtained by Boac et al. (2010). The mean corn moisture content of 15.2% (range of 14.9% to 16.1%) was within the typical corn moisture content at harvest maturity of 15% to 25% (Nielsen, 2008; Abendroth et al., 2009). The mean coefficients of restitution for corn-to-corn ($e_{\text{corn:corn}} = 0.25$), corn-to-acrylic ($e_{\text{corn:wall}} = 0.57$), and corn-to-stainless steel ($e_{\text{corn:wall}} = 0.61$) interactions were obtained from the single-particle dropping tests. The values estimated with the drop tests were within the ranges reported by Boac et al. (2010) and González-Montellano et al. (2012).

Bucket Test AOR

The mean bucket-discharged AOR (α_{bucket}), as estimated from the middle corn height profile, was 21.1° (standard deviation of 1.5° and sample size = 5). The AOR from the bucket test described the quasi-static grain flow from emptying the bucket. As the grain flowed along the 250 mm length and 120 mm width of the bucket, the AOR was influenced by the effects of grain-to-grain and grain-to-wall friction. The mean AOR from the bucket test was slightly lower than the range (23.1° to 34.7°) reported by Boac et al. (2010). This could be associated with the relatively lower static and rolling resistance of corn sliding along the acrylic walls.

Anchor Test AOR

The measured anchor-lifted AOR (α_{anchor}) was 29.8° (standard deviation of 3.5° and sample size = 5). From the experimental tests, α_{anchor} was approximately 1.4 times higher than α_{bucket} from the bucket test. The higher anchor AOR than bucket AOR showed that corn-to-corn friction (sliding and rolling) behaviors dominated the anchor test. As shown in the AOR data from the two calibration experiments (fig. 5), the grain flow multi-responses constituted the associated AOR values affected by the angle of internal friction of corn-to-corn friction from the anchor test and the angle of internal friction of corn-to-corn and corn-to-acrylic friction from the bucket test. Having such multi-responses makes the

two calibration experiments good candidates for the DEM calibration methodology of dynamic corn flow.

Auger Test

The steady-state mass flow rate was measured as 1.52 kg s⁻¹ (standard deviation of 0.023, sample size = 3, and $R^2 = 0.9996$) and 2.38 kg s⁻¹ (standard deviation of 0.075, sample size = 3, and $R^2 = 0.9986$) for the 250 and 450 rpm auger speeds, respectively.

DEM SENSITIVITY AND CALIBRATION

Figures 6 and 7 show the MSE values from the 27 DEM runs of the bucket and anchor AOR tests, respectively, for 1-sphere, 2-spheres, 5-spheres, and 13-spheres. For a similar combination of DEM parameters (27 DEM simulations), the DEM shape representations showed noticeable differences in MSE magnitude and distribution for bucket AOR (fig. 6) and anchor AOR (fig. 7). With the high-fidelity and computationally expensive 5-spheres and 13-spheres corn models, the differences in MSE were minimal.

Using the laboratory-measured corn height (h_{exp} in eq. 1) as a 95% confidence interval (mean of 8.6 mm and range of 6.6 to 19.9 mm) for the error between DEM and laboratory-measured height ($h_s - h_{\text{exp}}$ in eq. 1), within the 20% percentile of the height error, there were minimal differences among the results for 2-spheres, 5-spheres, and 13-spheres (fig. 8a). The computational effort required to run the DEM bucket simulations for 5-spheres and 13-spheres was approximately twice and three times, respectively, the effort required for the 2-spheres DEM bucket simulations. The 1-sphere model had the lowest computational effort (0.1 h per simulation) but higher MSE than 2-spheres at the corresponding DOE settings.

From the anchor DOE simulations, the 2-spheres and 13-spheres models showed lower percentiles (fig. 8b) of mean AOR errors ($\text{AOR}_s - \text{AOR}_{\text{exp}}$ in eq. 2), less than the one standard deviation of the laboratory-measured AOR (3.5°). Detailed corn shape approximations, such as the 13-spheres model, could be considered a good option for small-scale simulations of grain-to-equipment interaction; however, simulating large grain handling applications using the 13-spheres corn model would be computationally expensive.

Based on the lower computational effort and lower percentiles of MSE for bucket AOR and anchor AOR, the 2-spheres DEM corn model was chosen as the best shape approximation for DEM parameter calibration and validation of grain flow in a grain auger. The two best stepwise regression meta-models from the 2-spheres DOE relationship between DEM parameters and MSE with p-values between 0.05 and 0.1 were selected for the bucket AOR MSE ($R^2 = 0.9423$ and RMSE = 94.56) and anchor AOR MSE ($R^2 = 0.5412$ and RMSE = 78.02).

Sensitivity of DEM Friction Coefficients and Calibration of 2-Spheres Model

The two interaction effects of the DEM particle-to-particle coefficients (CC_{stat} and CC_{roll}) significantly affected the MSE for bucket AOR ($p = 0.0171$). The minimum MSE for bucket AOR was observed at the low settings of CC_{stat}

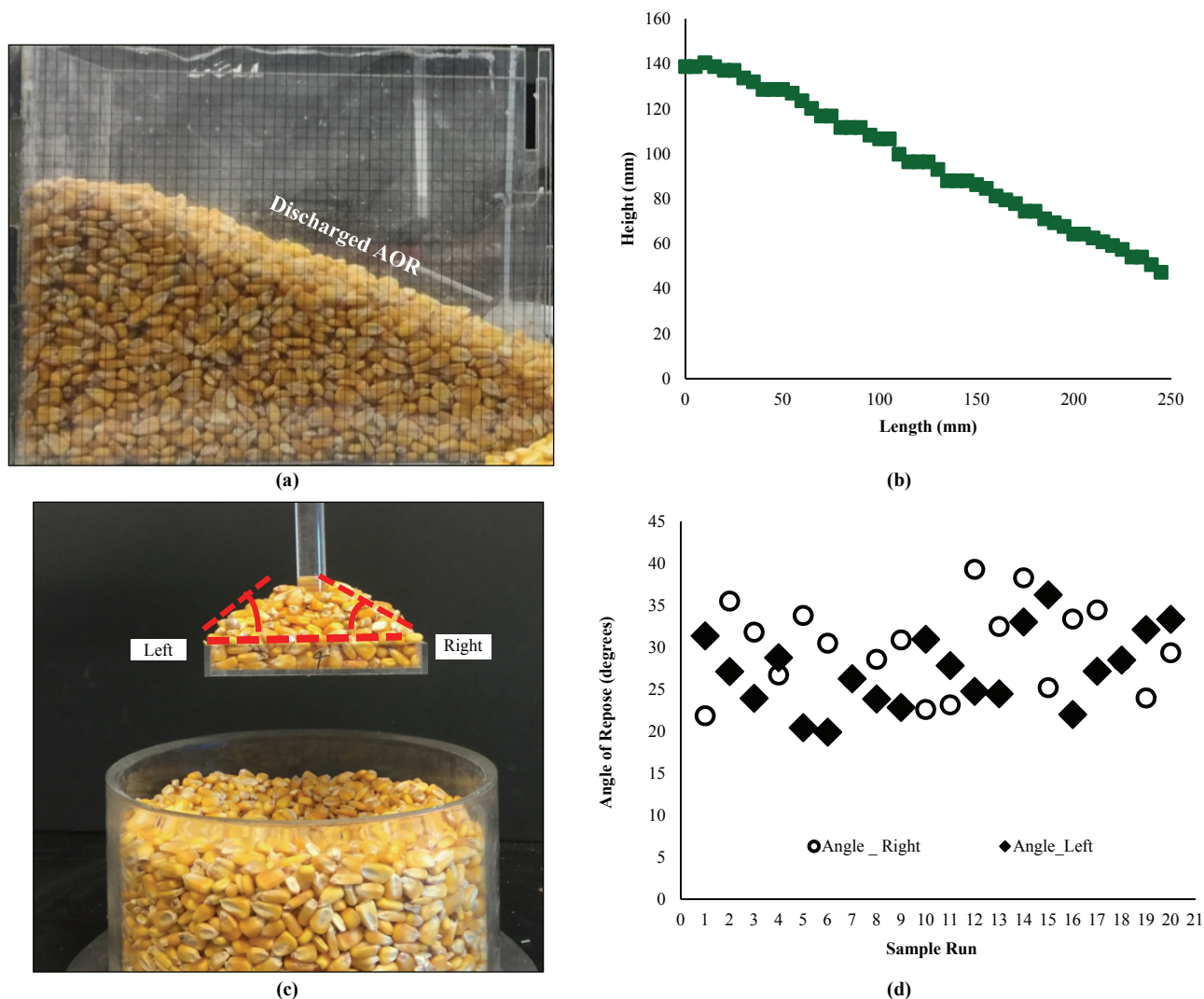


Figure 5. (a) Corn AOR from bucket test (α_{bucket}) showing discharged AOR and (b) mean free-surface profile (sample size = 5) along the bucket length, and (c) corn AOR from anchor test (α_{anchor}) showing lifted AOR and (d) measured AOR from the left and right sides of the anchor.

(0.1) and CC_{roll} (0.0). At the high setting of CC_{roll} (0.1), an increase in CC_{stat} from 0.1 to the high setting ($CC_{\text{stat}} = 0.55$) resulted in a significant increase in MSE. The corn-to-acrylic coefficient of static friction (CA_{stat}) showed a significant ($p < 0.0001$) effect on the MSE for bucket AOR; however, the corn-to-acrylic rolling friction coefficient (CA_{roll}) was not statistically significant ($p = 0.0633$). Except for the two-way interaction effects of CC_{stat} and CC_{roll} , all other possible two-way interaction effects of particle-to-particle and particle-to-wall coefficients were not significant ($p > 0.05$) in influencing the MSE.

Using the 27 DEM training parameters as independent variables, the MSE from the bucket AOR tests as the dependent variable, and the criterion of p-values between 0.05 and 0.1, a best stepwise regression model ($R^2 = 0.94$ and $RMSE = 94.56$) was developed to predict the MSE of bucket AOR. The stepwise regression model for the MSE of bucket AOR included the parameter estimates of intercept, CC_{stat} , CC_{roll} , and CA_{stat} and the two-way interactions effects of CC_{stat} and CC_{roll} .

The sensitivity of DEM parameters on the MSE of the

anchor AOR tests showed that none of the particle-to-wall parameters (CA_{stat} and CA_{roll}) and two-way interaction effects significantly ($p > 0.05$) influenced the anchor AOR. The particle-to-particle coefficients, CC_{stat} ($p < 0.0001$) and CC_{roll} ($p = 0.0114$), significantly affected the MSE for anchor AOR. For the anchor AOR tests, the results showed the influence of only corn-to-corn parameters on bulk AOR formation. A best-fit regression meta-model for MSE was fit using CC_{stat} and CC_{roll} as independent parameters with p-values between 0.05 and 0.1. The particle-to-wall static coefficient of friction (CC_{stat}) was added later even though its effect on MSE was not significant ($p = 0.87$) because the prediction profiler had to estimate the value of CC_{stat} to approximate the multi-responses for MSE for both bucket AOR and anchor AOR. The regressed meta-model for the MSE of anchor AOR with the parameter estimates of intercept, CC_{stat} , CC_{roll} , CA_{stat} , and two-way interactions effects of CC_{stat} and CC_{roll} had $R^2 = 0.54$ and $RMSE = 78.02$.

Using the best-fitting stepwise meta-models for MSE from the bucket and anchor AOR tests, 5,000 random DEM

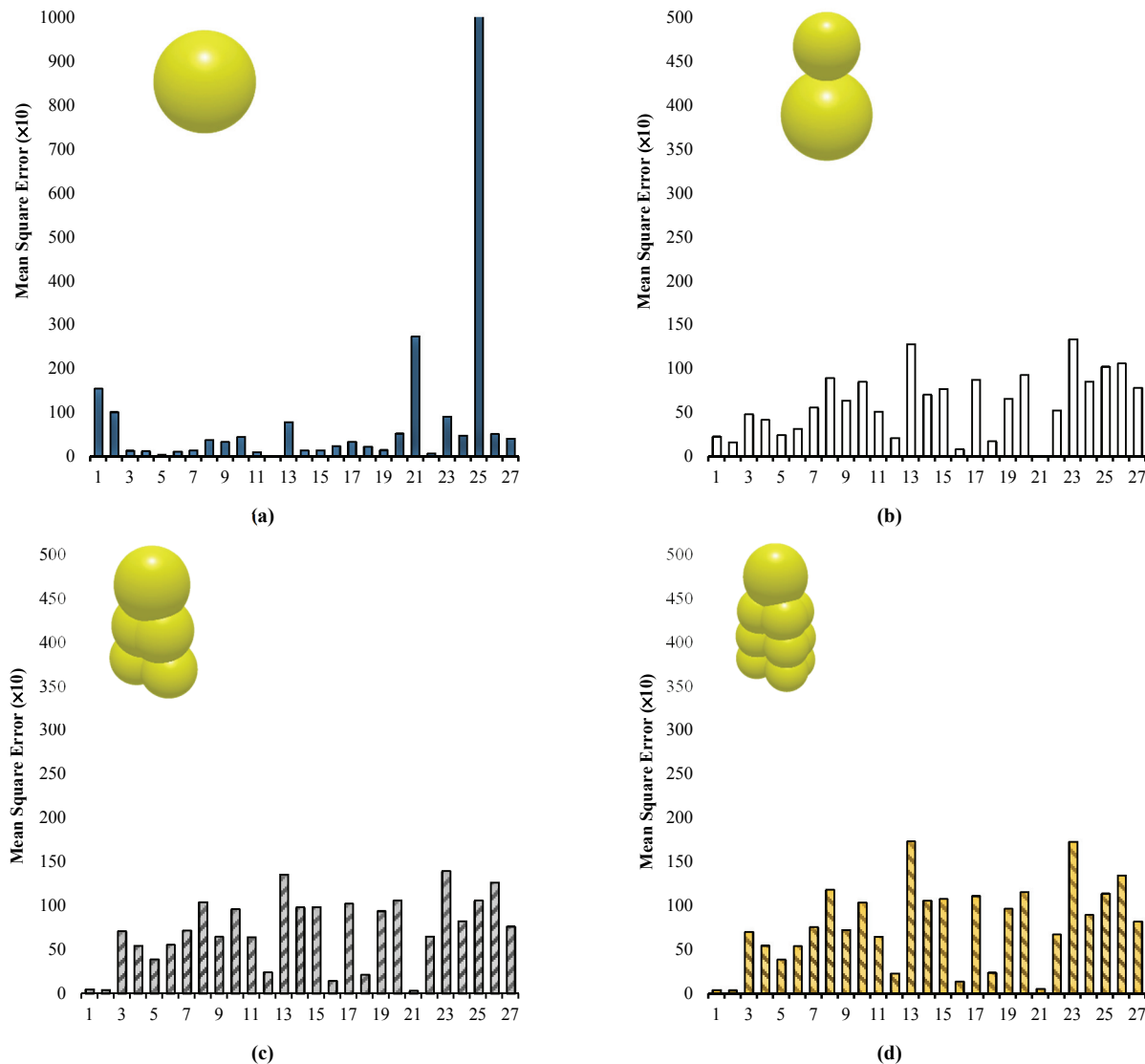


Figure 6. Mean square error from 27 DEM simulations of bucket AOR tests for (a) 1-sphere, (b) 2-spheres, (c) 5-spheres, and (d) 13-spheres.

input combinations of independent and dependent (MSE) responses were used to generate the fitting surface response to find the optimal DEM interaction parameter values that provided the minimum MSE for the two bulk responses of AOR from the bucket and anchor tests. The prediction profiler desirability function in JMP Pro 12 (SAS Institute Inc., Cary, N.C.) with the minimum MSE for bucket AOR and anchor AOR was used to obtain the optimal DEM input parameters (fig. 9). Tables 2 and 3 show the calibrated DEM model input parameters for corn-to-corn and corn-to-acrylic for the 2-spheres DEM model.

EDEM simulations of the bucket and anchor AOR tests were run using the optimal DEM parameters estimated from the prediction profiler using the two regression meta-models for bucket AOR MSE ($R^2 = 0.94$ and $RMSE = 94.56$) and anchor AOR MSE ($R^2 = 0.54$ and $RMSE = 78.02$). The DEM-predicted AOR values from the bucket and anchor simulations were 22.9° and 31.9° , respectively. Compared with the mean laboratory-measured values (bucket AOR of 21.1° and anchor AOR of 29.8°), the corresponding relative errors were 8.5% for bucket AOR and 7.0% for anchor AOR.

Validation of DEM Corn Model

The mass flow rate of corn through the auger and the shape of the corn pile discharged from the auger onto the flat stainless-steel plate were used as responses to validate the DEM simulations against the laboratory tests. The DEM-predicted steady-state mass flow rates of corn through the auger at speeds of 250 and 450 rpm were 1.39 and 2.41 kg s^{-1} , respectively. The DEM prediction errors compared to the measured steady-state mass flow rates of 1.52 kg s^{-1} at 250 rpm and 2.38 kg s^{-1} at 450 rpm were 8.55% and 1.26%, respectively. The differences between the DEM-predicted and laboratory-measured values were not statistically significant ($p = 0.6444$). As the auger speed increased from 250 to 450 rpm, the steady-state mass flow rate increased by 1.7 times in the laboratory tests and by 1.6 times in the DEM simulations. For the magnitude and trend in mass flow rate, the calibrated DEM model showed good agreement with the laboratory data.

The DEM model also showed good agreement with the qualitative flow of grain from the auger outlet and onto the static pile (fig. 10). The static AOR values estimated using

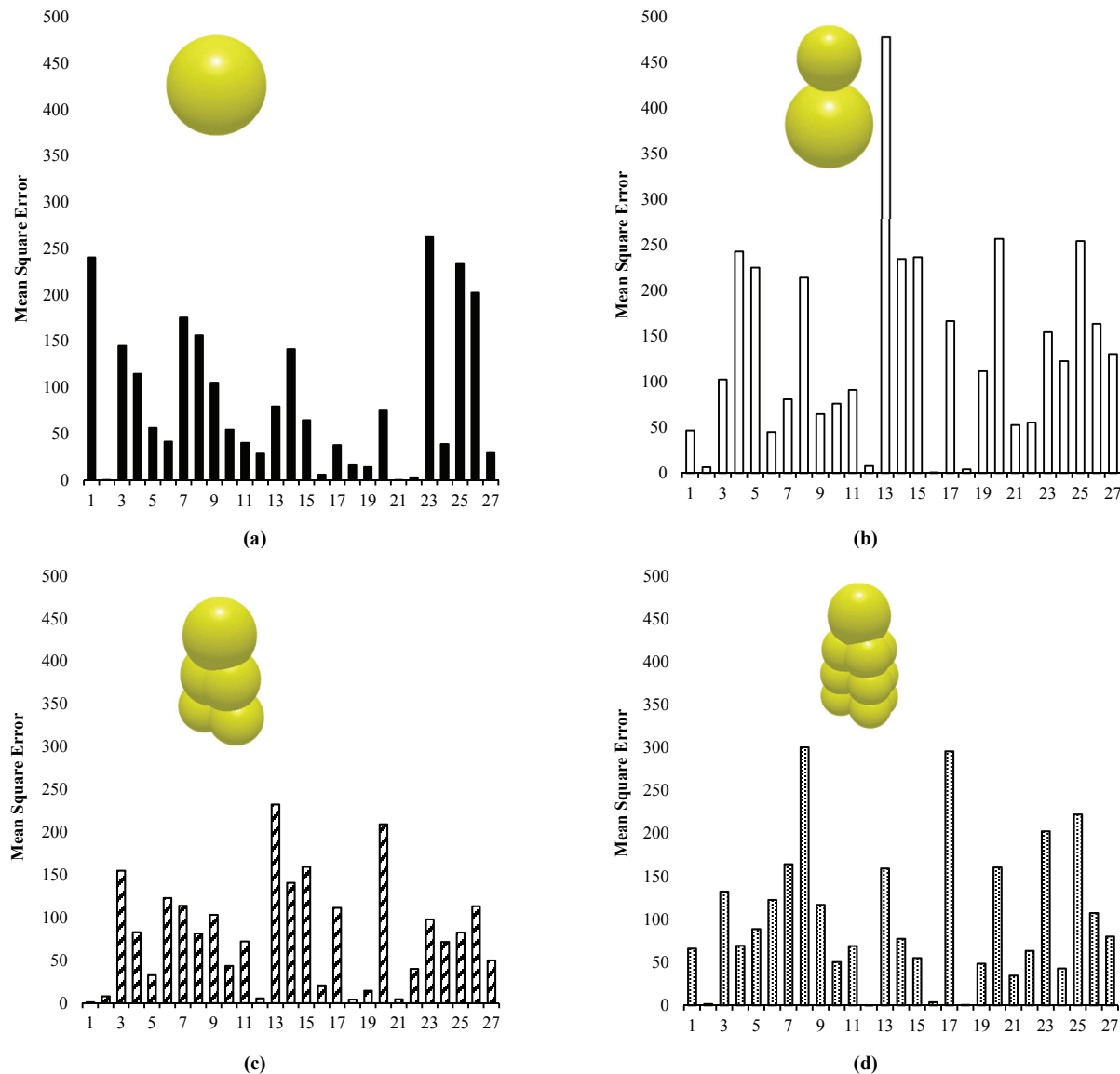


Figure 7. Mean square error from 27 DEM simulations of anchor AOR tests for (a) 1-sphere, (b) 2-spheres, (c) 5-spheres, and (d) 13-spheres.

Matlab image processing of high-speed camera images (240 fps) and EDEM post-processing are listed in table 4. The static AOR was estimated at four corn masses (10, 20, 30, and 40 kg) as discharged onto the stainless-steel surface. The DEM prediction errors compared to the laboratory measurements ranged from 2.8% to 6.9% ($p = 0.2855$) for 250 rpm and from 5.7% to 9.6% ($p = 0.6627$) for 450 rpm among the four pile masses. The differences between the DEM-predicted and mean measured values for steady-state mass flow and static AOR in the auger tests were not statistically significant ($p > 0.05$). This indicates that the calibrated DEM corn model was quantitatively validated.

Previous studies have shown the qualitative prediction of granular flow through auger systems (McBride and Cleary, 2009; Shimizu and Cundall, 2001) but did not demonstrate quantitative prediction errors as low as 10%. Most previous DEM simulations of granular grain augers used a DEM simulation of the application, e.g., McBride and Cleary (2009) adjusted the input DEM properties until

the simulation matched the grain auger performance variables. Similarly, Fernandez et al. (2011) used DEM simulation of a grain auger application to obtain DEM properties that agreed with the experimental results before using the DEM for virtual screw blade designs. Using a calibration approach with a single bulk response from bucket AOR tests to obtain the minimum MSE (Mousaviraad et al., 2017), the DEM predicted the steady-state mass flow rate with prediction errors of 27% and 29% for 250 and 450 rpm, respectively. The underprediction of steady-state mass flow rate might have been due to limitations in capturing particle-to-particle friction behaviors (sliding and rolling). In the current study, in addition to the bucket-discharged AOR test, an anchor-lifted AOR test was added to provide multi-response calibration. The improved DEM calibration using these simple laboratory tests and a validation methodology for corn showed significant improvement for the calibrated DEM-predicted mass flow rate from the auger, with prediction errors of 8.55% and 1.26% for

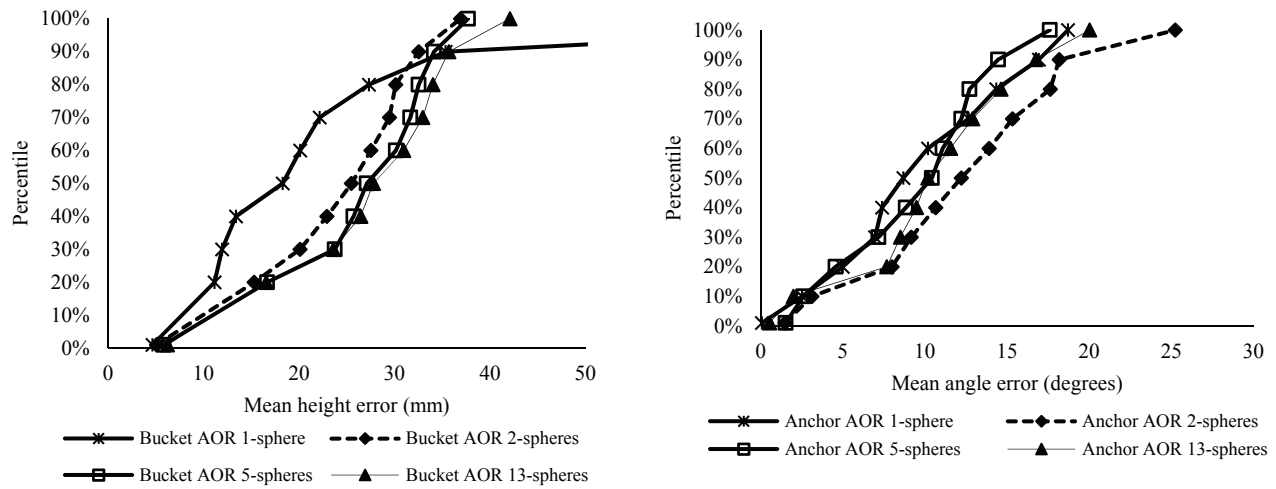


Figure 8. Percentiles of (a) mean height error (mm) from bucket AOR test and (b) mean angle error (degrees) from anchor AOR test for the 27 DEM simulations using 1-sphere, 2-spheres, 5-spheres, and 13-spheres.

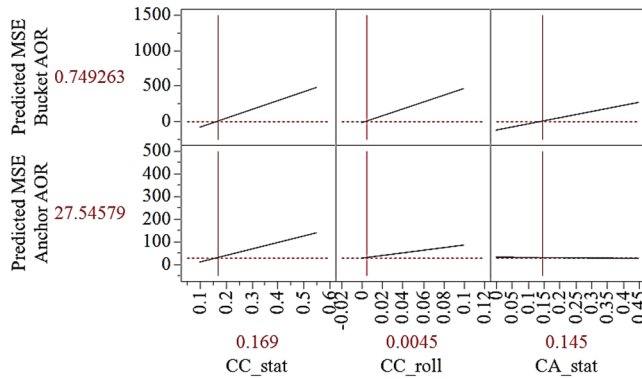


Figure 9. Meta-model prediction profiler estimates of DEM friction coefficients (CC-stat, CC-roll, and CA-stat) to minimum predicted MSE values for bucket AOR and anchor AOR. The meta-model used the relationship shown in table 2.

auger speeds of 250 and 450 rpm, respectively. With the multi-response calibrated DEM using the 2-spheres corn model, the static AOR of piled grain discharged from the grain auger at 250 and 450 rpm was predicted with maximum relative errors of 6.9% to 9.6%, respectively.

CONCLUSIONS

A laboratory methodology for calibration of a discrete element model (DEM) of corn was developed, including material characterization, a method for approximating the DEM corn shape, and multi-response calibration of static and rolling friction interaction parameters. The multi-response angle of repose (AOR) from bucket-discharged tests and anchor-lifted tests was successfully used to show the sensitivity of DEM friction interaction parameters for 1-sphere, 2-spheres, 5-spheres, and 13-spheres corn models to simulate the AOR.

A Latin hypercube design of experiments (DOE) and stepwise regression modeling were used to choose representative sample points from the input domain and predict the mean square error (MSE) of the AOR from the bucket and anchor tests. The calibrated DEM corn model was validated by comparing the predicted steady-state mass flow rate and the static AOR of the discharged corn pile from auger simulations. The DEM simulation of corn flow in the auger showed very good agreement in (1) qualitative comparison with the grain flow in laboratory images captured at 240 fps and (2) quantitative prediction of the mass flow rate (within 10% error) and static AOR of discharged corn at 250 and 450 rpm grain auger speeds. With this quantitatively validated simulation of corn flow in a grain auger, future research will be possible to predict the relationship between grain mass flow rate and grain auger variables, such as rotational speed and screw diameter.

Table 2. Calibrated DEM interaction parameters using the stepwise regression meta-model analysis of bucket AOR MSE ($R^2 = 0.94$ and RMSE of 94.56) and anchor AOR MSE ($R^2 = 0.54$ and RMSE = 78.02).

Parameter	Material	Interaction Material			
		Corn	Acrylic	Smooth Steel ^[a]	Steel Plate ^[b]
Coefficient of static friction	Corn	0.169	0.145	0.145	0.23
Coefficient of rolling friction	Corn	0.0045	0.1	0.1	0.1
Coefficient of restitution	Corn	0.2	0.67	0.67	0.67

^[a] The auger screw shaft and tube surfaces were smooth, and corn-to-steel coefficients of static and rolling friction were assumed similar to the calibrated corn-to-acrylic static and rolling coefficients, based on the ratio of the coefficients of restitution of corn-to-acrylic and corn-to-smooth steel.

^[b] The steel plate on which the corn pile was measured in the auger test had a rough surface, and a value 1.58 higher than the coefficient of corn-to-acrylic was used, after Boac et al. (2010).

Table 3. DEM material properties.

Material	Parameter	DEM
Corn	Particle density (kg m^{-3}) ^[a]	1280
	Shear modulus (MPa) ^[b]	1.071
	Poisson's ratio ^[b]	0.4
Acrylic ^[c]	Density (kg m^{-3})	1180
	Shear modulus (MPa)	1100
	Poisson's ratio	0.35
Steel ^[d]	Density (kg m^{-3})	7800
	Shear modulus (GPa)	70
	Poisson's ratio	0.3

[a] Calibrated to match initial bulk density.

[b] Boac et al. (2010).

[c] From the Acrylite FF material datasheet.

[d] Properties for steel are from the EDEM 2.7 default database.

Table 4. The angle of repose of corn discharged from auger outlet onto flat stainless-steel plate. The DEM angle of repose data were obtained from simulations using the calibrated DEM properties.

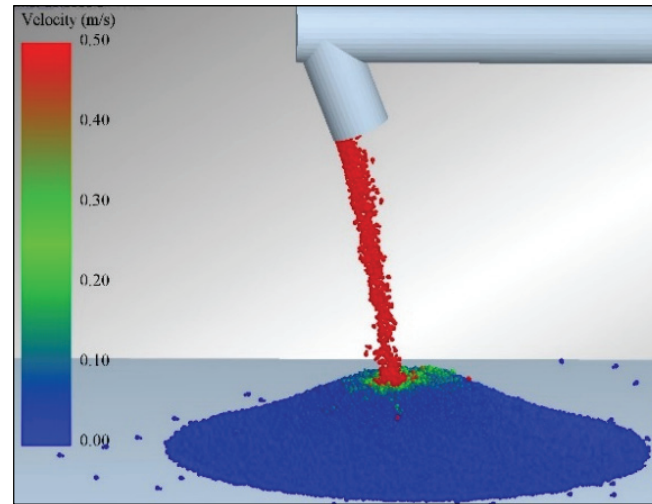
Corn Pile Mass (kg)	Grain Auger Rotational Speed (rpm)	Angle of Repose (degrees)	
		Test	DEM
10	250	20.3	19.6
20	250	24.7	23.0
30	250	25.0	23.9
40	250	25.1	24.4
10	450	15.8	16.7
20	450	22.8	20.6
30	450	23.9	23.3
40	450	24.0	23.5



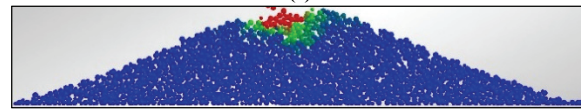
(a)



(b)



(c)



(d)

Figure 10. (a) Corn (20 kg) discharged from grain auger (250 rpm) outlet, (b) image processed corn pile, and (c and d) DEM simulations.

REFERENCES

- Abendroth, L., Elmore, R., Hartzler, R. G., McGrath, C., & Mueller, D. S. (2009). Corn field guide. Publication 26. Ames, IA: Iowa State University Extension and Outreach.
- ASABE. (2006). S352.2: Moisture measurement - Unground grain and seeds. St. Joseph, MI: ASABE.
- Asaf, Z., Rubinstein, D., & Shmulevich, I. (2007). Determination of discrete element model parameters required for soil tillage. *Soil Tillage Res.*, 92(1), 227-242. <https://doi.org/10.1016/j.still.2006.03.006>
- ASTM. (2000). D854: Standard test methods for specific gravity of soil solids by water pycnometer. West Conshohocken, PA: ASTM.
- Boac, J. M., Casada, M. E., Maghirang, R. G., & Harner III, J. P. (2010). Material and interaction properties of selected grains and oilseeds for modeling discrete particles. *Trans. ASABE*, 53(4), 1201-1216. <https://doi.org/10.13031/2013.32577>
- Chen, Y., Munkholm, L. J., & Nyord, T. (2013). A discrete element model for soil sweep interaction in three different soils. *Soil Tillage Res.*, 126, 34-41. <https://doi.org/10.1016/j.still.2012.08.008>
- Cleary, P. W. (2013). Particulate mixing in a plough share mixer using DEM with realistic shaped particles. *Powder Tech.*, 248, 103-120. <https://doi.org/10.1016/j.powtec.2013.06.010>
- Coetzee, C. J. (2016). Calibration of the discrete element method and the effect of particle shape. *Powder Tech.*, 297, 50-70. <https://doi.org/10.1016/j.powtec.2016.04.003>
- Coetzee, C. J. (2017). Review: Calibration of the discrete element method. *Powder Tech.*, 310, 104-142. <https://doi.org/10.1016/j.powtec.2017.01.015>
- Coetzee, C. J. J., & Els, D. N. J. N. J. (2009a). Calibration of discrete element parameters and the modeling of silo discharge and bucket filling. *Comput. Electron. Agric.*, 65(2), 198-212. <https://doi.org/10.1016/j.compag.2008.10.002>
- Coetzee, C. J. J., & Els, D. N. J. N. J. (2009b). Calibration of granular material parameters for DEM modeling and numerical verification by blade-granular material interaction. *J. Terramech.*, 46(1), 15-26. <https://doi.org/10.1016/j.jterra.2008.12.004>
- Coetzee, C. J. J., Els, D. N. J. N. J., & Dymond, G. F. (2010). Discrete element parameter calibration and the modeling of dragline bucket filling. *J. Terramech.*, 47(1), 33-44. <https://doi.org/10.1016/j.jterra.2009.03.003>
- Cundall, P. A., & Strack, O. D. L. A. (1979). A discrete numerical model for granular assemblies. *Geotechnique*, 29(1), 47-65. <https://doi.org/10.1680/geot.1979.29.1.47>
- EDEM. (2014). EDEM version 2.8. Edinburgh, UK: DEM Solutions.
- Fernandez, J. W., Cleary, P. W., & McBride, W. (2011). Effect of

- screw design on hopper drawdown of spherical particles in a horizontal screw feeder. *Chem. Eng. Sci.*, 66(22), 5585-5601. <https://doi.org/10.1016/j.ces.2011.07.043>
- González-Montellano, C., Fuentes, J. M., Ayuga-Téllez, E., & Ayuga, F. (2012). Determination of the mechanical properties of maize grains and olives required for use in DEM simulations. *J. Food Eng.*, 111(4), 553-562. <https://doi.org/10.1016/j.jfoodeng.2012.03.017>
- Kalala, J. T., Bwalya, M. M., & Moys, M. H. (2005). Discrete element method (DEM) modeling of evolving mill liner profiles due to wear: Part I. DEM validation. *Miner. Eng.*, 18(15), 1386-1391. <https://doi.org/10.1016/j.mineng.2005.02.009>
- Kretz, D., Callau-Monje, S., Hitschler, M., Hien, A., Raedle, M., & Hesser, J. (2016). Discrete element method (DEM) simulation and validation of a screw feeder system. *Powder Tech.*, 287, 131-138. <https://doi.org/10.1016/j.powtec.2015.09.038>
- Markauskas, D., Ramiez-Gomez, A., Kacianauskas, R., & Zdancevicius, E. (2015). Maize grain shape approaches for DEM modeling. *Comput. Electron. Agric.*, 118, 247-258. <https://doi.org/10.1016/j.compag.2015.09.004>
- McBride, W., & Cleary, P. W. (2009). An investigation and optimization of the "OLDS" elevator using discrete element modeling. *Powder Tech.*, 193(3), 216-234. <https://doi.org/10.1016/j.powtec.2009.03.014>
- Miao, Z., Grift, T. E., Hansen, A. C., & Ting, K. C. (2014). Flow performance of ground biomass in a commercial auger. *Powder Tech.*, 267, 354-361. <https://doi.org/10.1016/j.powtec.2014.07.038>
- Mohsenin, N. N. (1986). *The physical properties of plant and animal materials: Structure, physical properties, and mechanical properties*. New York, NY: Gordon and Breach.
- Mousaviraad, M., Tekeste, M. Z., & Rosentrater, K. A. (2017). Calibration and validation of a discrete element model of corn using grain flow simulation in a commercial screw grain auger. *Trans. ASABE*, 60(4), 1403-1415. <https://doi.org/10.13031/trans.12200>
- Nielsen, R. L. (2008). Grain fill stages in corn. West Lafayette, IN: Purdue University, Department of Agronomy. Retrieved from www.agry.purdue.edu/ext/corn/news/timeless/GrainFill.html
- Owen, P. J., & Cleary, P. W. (2009). Prediction of screw conveyor performance using the discrete element method (DEM). *Powder Tech.*, 193(3), 274-288. <https://doi.org/10.1016/j.powtec.2009.03.012>
- Risius, N. W. (2014). Analysis of a combine grain yield monitoring system. MS thesis. Ames, IA: Iowa State University, Department of Agricultural and Biosystems Engineering. Retrieved from <https://lib.dr.iastate.edu/cgi/viewcontent.cgi?article=4806&context=etd>
- Roberts, A. W. (2015). Bulk solids: Optimizing screw conveyors. *Chem. Eng.*, 122(2), 62-67.
- Roberts, A. W., & Willis, A. H. (1962). Performance of grain augers. *Proc. Inst. Mech Eng.*, 176(1), 165-194.
- Schulze, D. (2007). *Powders and bulk solids: Behavior, characterization, storage, and flow*. Berlin, Germany: Springer.
- Shimizu, Y., & Cundall, P. A. (2001). Three-dimensional DEM simulations of bulk handling by screw conveyors. *J. Eng. Mech.*, 127(9), 864-872. [https://doi.org/10.1061/\(ASCE\)0733-9399\(2001\)127:9\(864\)](https://doi.org/10.1061/(ASCE)0733-9399(2001)127:9(864))
- Srivastava, A. K. (2006). *Engineering principles of agricultural machines*. St. Joseph, MI: ASABE. <https://doi.org/10.13031/epam.2013>
- Stahl, M., & Konietzky, H. (2011). Discrete element simulation of ballast and gravel under special consideration of grain shape, grain size, and relative density. *Granular Matter*, 13(4), 417-428. <https://doi.org/10.1007/s10035-010-0239-y>
- Tsuji, Y., Tanaka, T., & Ishida, T. (1992). Lagrangian numerical simulation of plug flow of cohesionless particles in a horizontal pipe. *Powder Tech.*, 71(3), 239-250. [https://doi.org/10.1016/0032-5910\(92\)88030-L](https://doi.org/10.1016/0032-5910(92)88030-L)
- Ucugul, M., Fielke, J. M., & Saunders, C. (2014). Three-dimensional discrete element modeling of tillage: Determination of a suitable contact model and parameters for a cohesionless soil. *Biosyst. Eng.*, 121, 105-117. <https://doi.org/10.1016/j.biosystemseng.2014.02.005>
- Walton, O. R., & Braun, R. L. (1993). Simulation of rotary-drum and repose tests for frictional spheres and rigid sphere clusters. *Proc. Joint DOE/NSF Workshop on Flow of Particulates and Fluids*. Washington, DC: U.S. Department of Energy.
- Wiacek, J., Molenda, M., Horabik, J., & Ooi, J. Y. (2012). Influence of grain shape and intergranular friction on material behavior in uniaxial compression: Experimental and DEM modeling. *Powder Tech.*, 217, 435-442. <https://doi.org/10.1016/j.powtec.2011.10.060>
- Zhang, X., & Vu-Quoc, L. (2002). A method to extract the mechanical properties of particles in collision based on a new elasto-plastic normal force-displacement model. *Mech. Mater.*, 34(12), 779-794. [https://doi.org/10.1016/S0167-6636\(02\)00181-3](https://doi.org/10.1016/S0167-6636(02)00181-3)